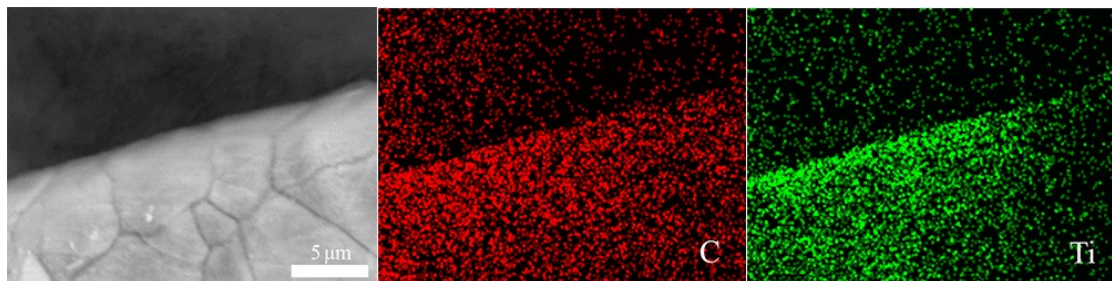
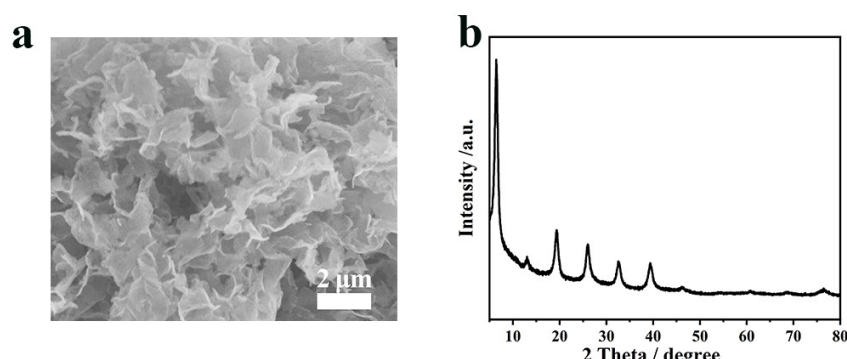


## Supplementary Information



**Fig. S1.** Element mapping images of MXene/NF.



**Fig. S2.** (a) SEM image of MXene. (b) XRD spectrum of MXene.

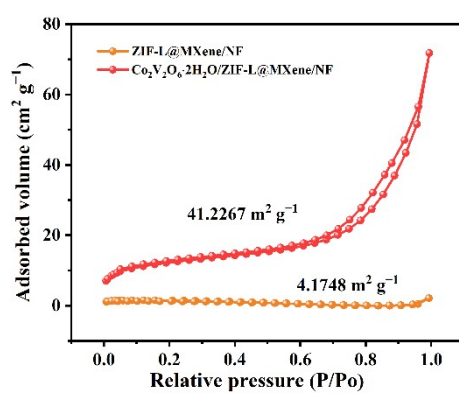


**Fig. S3.** Brunauer-Emmett-Teller isotherms of Co<sub>2</sub>V<sub>2</sub>O<sub>6</sub>·2H<sub>2</sub>O/ZIF-L@MXene/NF and ZIF-L@MXene/NF.

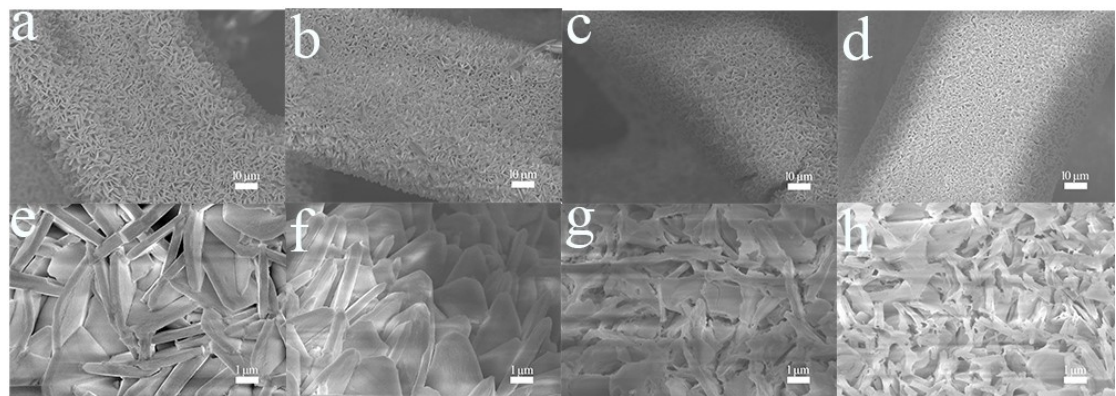


**Fig. S4.** SEM images of (a), (e)  $\text{Co}_2\text{V}_2\text{O}_6 \cdot 2\text{H}_2\text{O}/\text{ZIF-L}@\text{MXene}/\text{NF-5}$ , (b), (f)  $\text{Co}_2\text{V}_2\text{O}_6 \cdot 2\text{H}_2\text{O}/\text{ZIF-L}@\text{MXene}/\text{NF}$ , (c), (g)  $\text{Co}_2\text{V}_2\text{O}_6 \cdot 2\text{H}_2\text{O}/\text{ZIF-L}@\text{MXene}/\text{NF-15}$  and (d), (h)  $\text{Co}_2\text{V}_2\text{O}_6 \cdot 2\text{H}_2\text{O}/\text{ZIF-L}@\text{MXene}/\text{NF-20}$ .

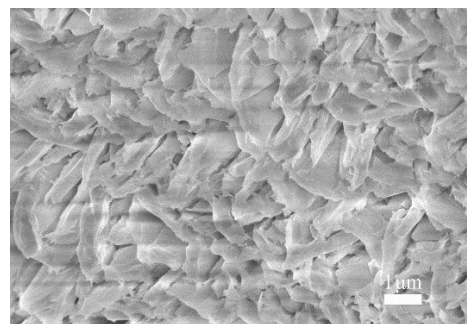


**Fig. S5.** SEM image of  $\text{Co}_2\text{V}_2\text{O}_6 \cdot 2\text{H}_2\text{O}/\text{ZIF-L}/\text{NF}$ .

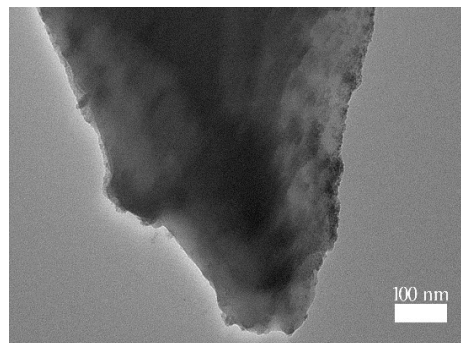


**Fig. S6.** TEM image of  $\text{Co}_2\text{V}_2\text{O}_6 \cdot 2\text{H}_2\text{O}/\text{ZIF-L}@\text{MXene}/\text{NF}$ .

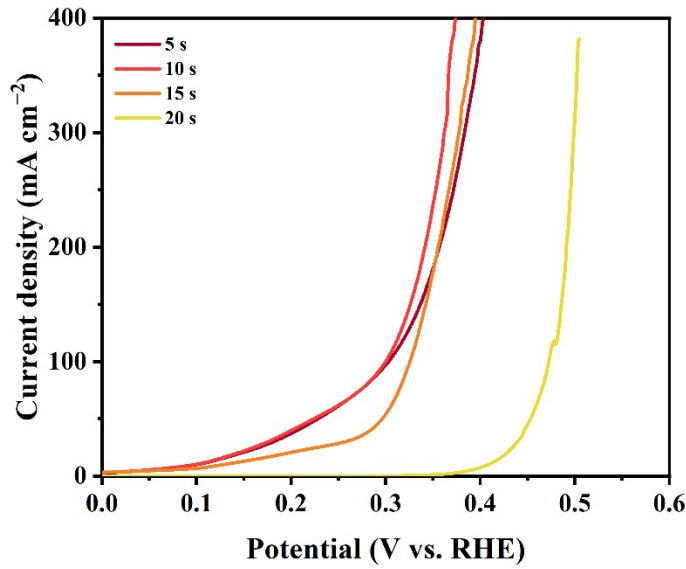


**Fig. S7.** OER performance: LSV polarization curves of  $\text{Co}_2\text{V}_2\text{O}_6 \cdot 2\text{H}_2\text{O}/\text{ZIF-L}@\text{MXene}/\text{NF}$  obtained by 5 s, 10 s, 15 s and 20 s reaction times.

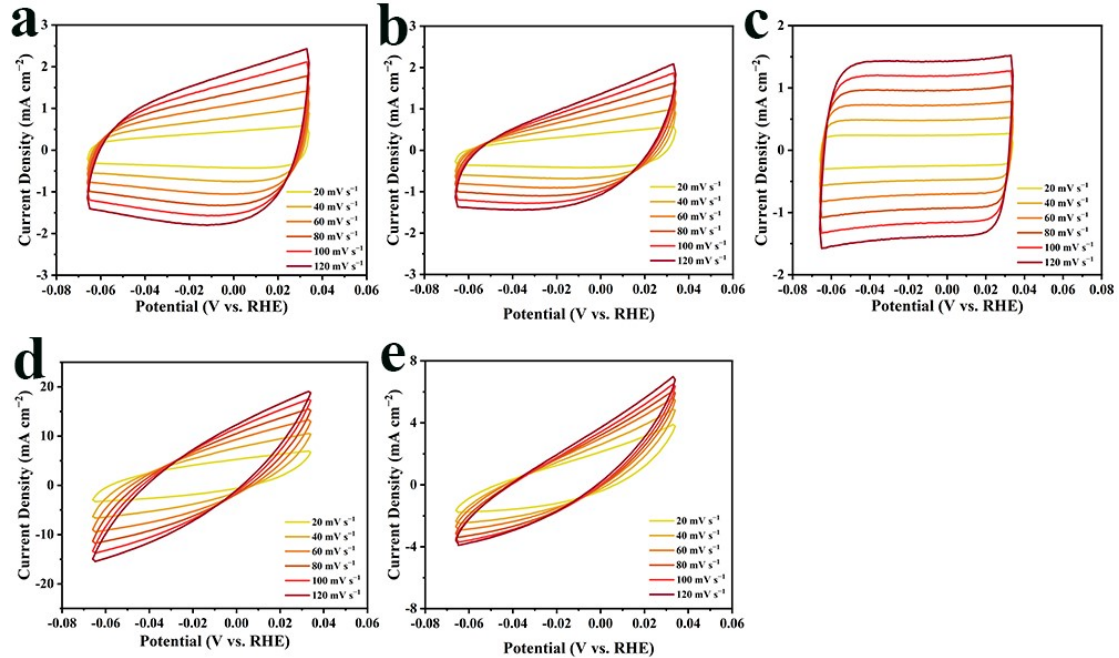


**Fig. S8.** OER performance: CV curves recorded at different scan rates within the non-Faradaic potential range for (a) NF, (b) MXene/NF, (c) ZIF-L@MXene/NF, (d)  $\text{Co}_2\text{V}_2\text{O}_6 \cdot 2\text{H}_2\text{O}/\text{ZIF-L}@\text{MXene}/\text{NF}$  and (e)  $\text{Co}_2\text{V}_2\text{O}_6 \cdot 2\text{H}_2\text{O}/\text{ZIF-L}/\text{NF}$ .

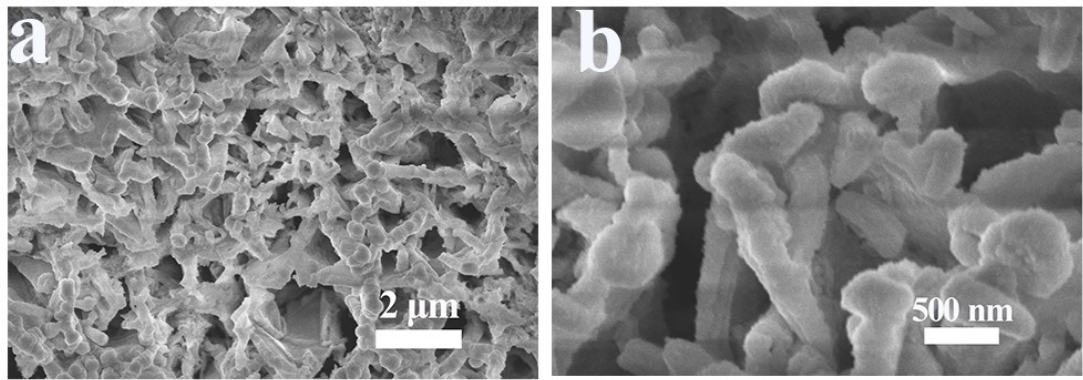


**Fig. S9.** SEM images of  $\text{Co}_2\text{V}_2\text{O}_6 \cdot 2\text{H}_2\text{O}/\text{ZIF-L}@\text{MXene}/\text{NF}$  after OER 1000 CV cycles.

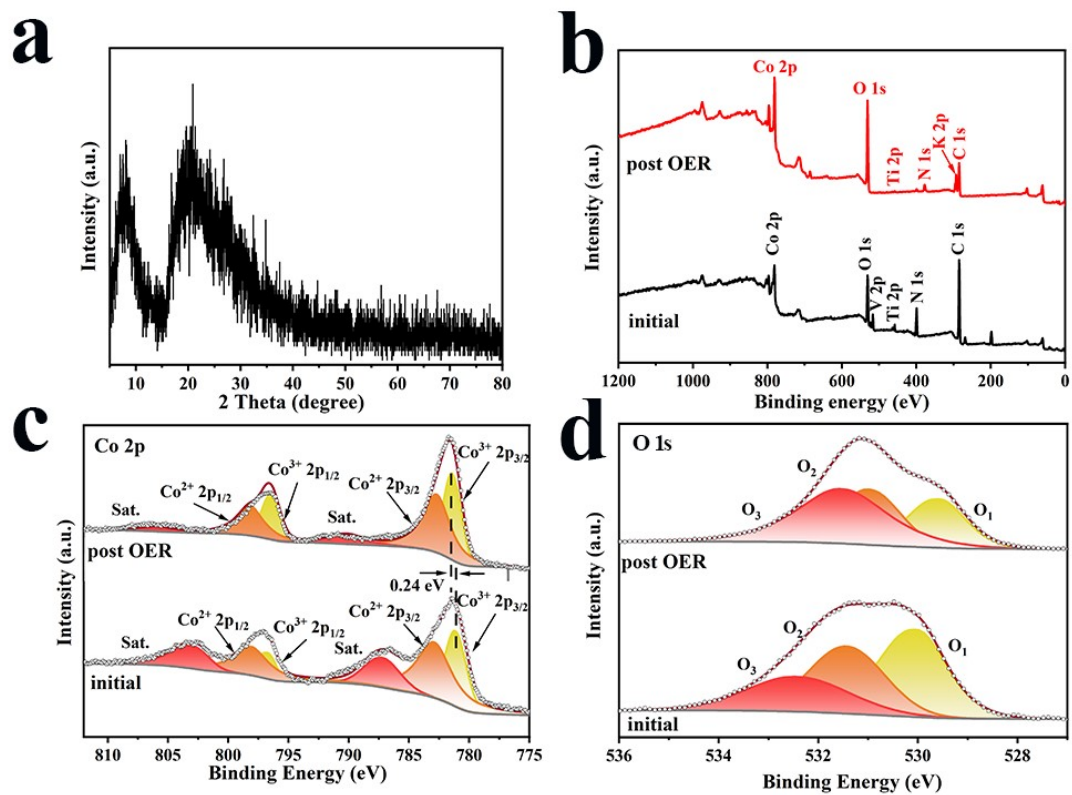


**Fig. S10.** (a) XRD spectrum of  $\text{Co}_2\text{V}_2\text{O}_6 \cdot 2\text{H}_2\text{O}/\text{ZIF-L}@\text{MXene}/\text{NF}$  before and after 1000 cycles. (b) XPS survey spectra of  $\text{Co}_2\text{V}_2\text{O}_6 \cdot 2\text{H}_2\text{O}/\text{ZIF-L}@\text{MXene}/\text{NF}$  before and after 1000 cycles. XPS spectra of (c) Co 2p and (d) O 1s of different catalysts before and after 1000 cycles.

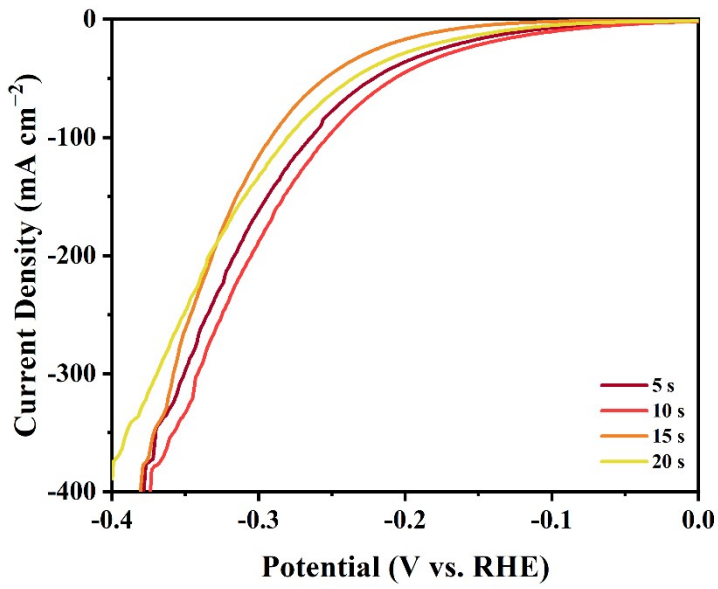


**Fig. S11.** HER performance: LSV polarization curves of  $\text{Co}_2\text{V}_2\text{O}_6 \cdot 2\text{H}_2\text{O}/\text{ZIF-L}@\text{MXene}/\text{NF}$  obtained at 5 s, 10 s, 15 s and 20 s reaction times.

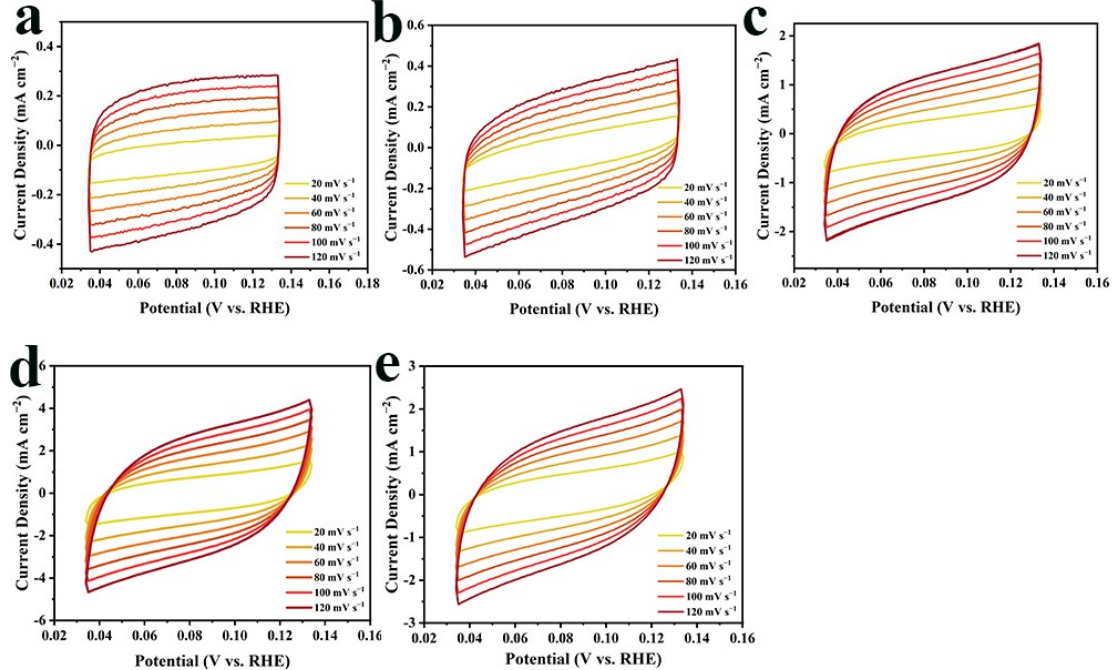


**Fig. S12.** HER performance: CV curves recorded at different scan rates within the non-Faradaic potential range for (a) NF, (b) MXene/NF, (c) ZIF-L@MXene/NF, (d)  $\text{Co}_2\text{V}_2\text{O}_6 \cdot 2\text{H}_2\text{O}/\text{ZIF-L}@\text{MXene}/\text{NF}$  and (e)  $\text{Co}_2\text{V}_2\text{O}_6 \cdot 2\text{H}_2\text{O}/\text{ZIF-L}/\text{NF}$ .

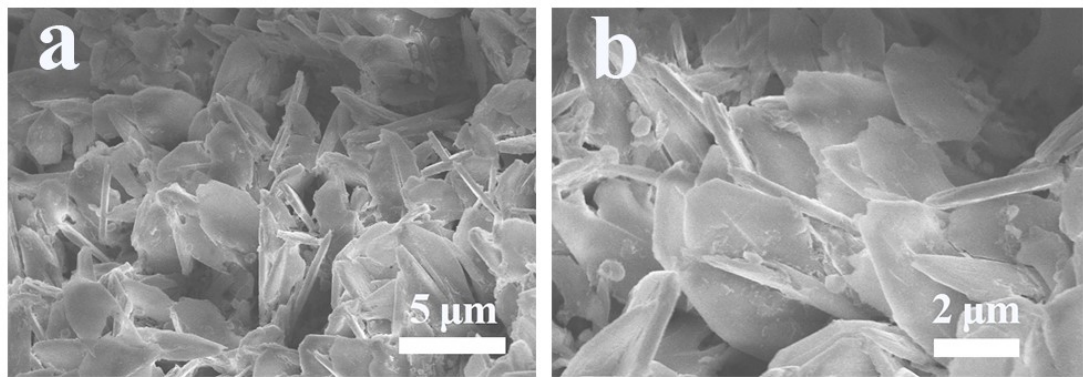


**Fig. S13.** SEM images of  $\text{Co}_2\text{V}_2\text{O}_6 \cdot 2\text{H}_2\text{O}/\text{ZIF-L}@\text{MXene}/\text{NF}$  after HER 1000 CV cycles.

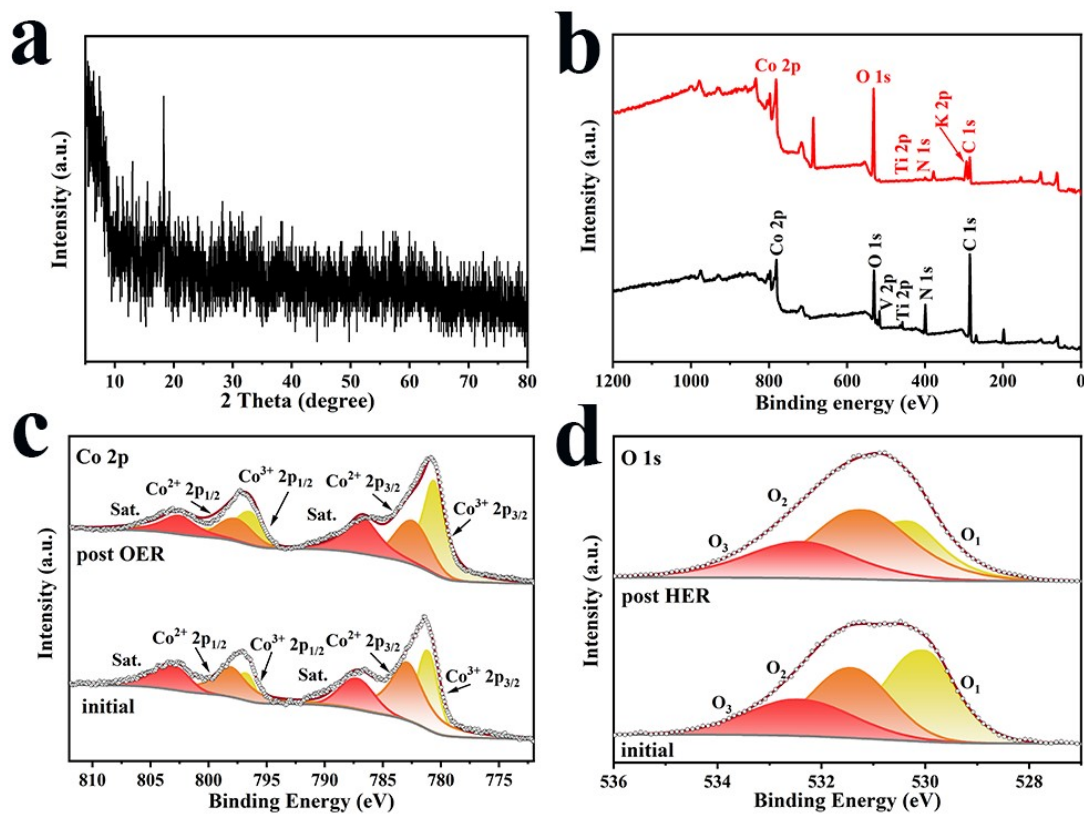


**Fig. S14.** (a) XRD spectrum of  $\text{Co}_2\text{V}_2\text{O}_6 \cdot 2\text{H}_2\text{O}/\text{ZIF-L}@\text{MXene}/\text{NF}$  before and after HER 1000 cycles. (b) XPS survey spectra of  $\text{Co}_2\text{V}_2\text{O}_6 \cdot 2\text{H}_2\text{O}/\text{ZIF-L}@\text{MXene}/\text{NF}$  before and after HER 1000 cycles. XPS spectra of (c) Co 2p and (d) O 1s of different catalysts before and after HER 1000 cycles.

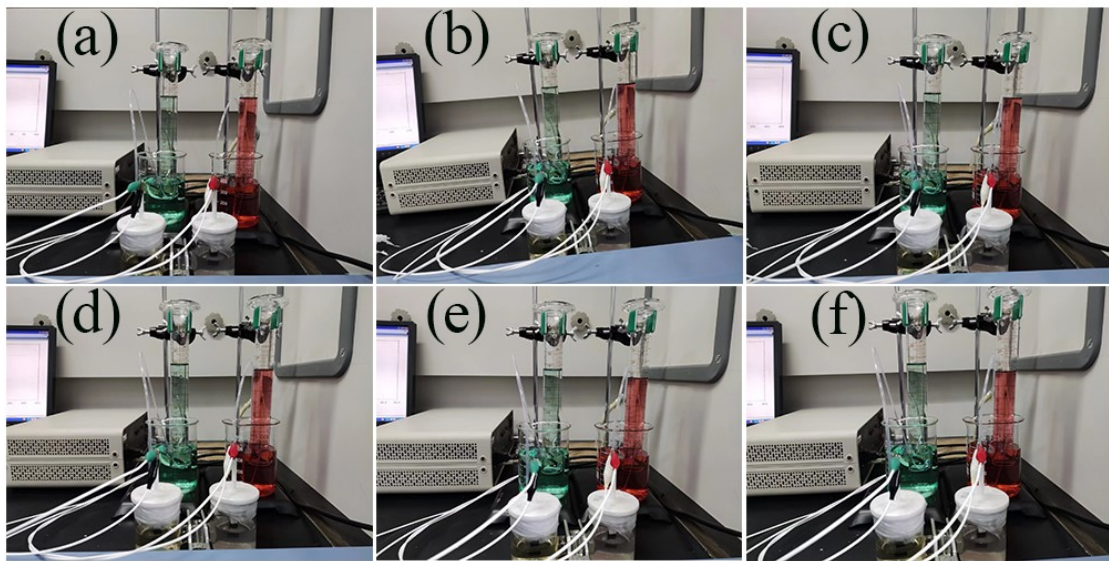


**Fig. S15.** Corresponding gas volume generated at (a) 0 s, (b) 400 s, (c) 800 s, (d) 1200 s, (e) 1600 s and (f) 2000 s.

**Table S1.** Comparison of the OER activities between  $\text{Co}_2\text{V}_2\text{O}_6 \cdot 2\text{H}_2\text{O}/\text{ZIF-L}@\text{MXene/NF}$  in this work and various electrocatalysts recently reported.

Materials	$\eta_{50}$ (mV)	Electrolyte	Ref
<b>This work</b>	224	1.0 M KOH	<b>This work</b>
<b>V-CoP</b>	300	1.0 M KOH	[1]
<b>Ru-CoV-LDH/NF</b>	290	1.0 M KOH	[2]
<b>CoV/CF-CWs</b>	230	1.0 M KOH	[3]
<b>Ti<sub>3</sub>C<sub>2</sub>T<sub>x</sub> MXene @NiCo<sub>2</sub>(OH)<sub>x-p</sub></b>	310	1.0 M KOH	[4]
<b>Ti<sub>3</sub>C<sub>2</sub>@SrTiO<sub>3</sub></b>	400	1.0 M KOH	[5]

**Table S2.** Comparison of the HER activities between  $\text{Co}_2\text{V}_2\text{O}_6 \cdot 2\text{H}_2\text{O}/\text{ZIF-L}@\text{MXene}/\text{NF}$  in this work and various electrocatalysts recently reported.

Materials	$\eta_{10}$ (mV)	Electrolyte	Ref
<b>This work</b>	98	1.0 M KOH	<b>This work</b>
$\text{Co}_3\text{O}_4/\text{Ti}_3\text{C}_2$ <b>MXene</b>	124	1.0 M KOH	[6]
$\text{NiFeP}/\text{Ti}_3\text{C}_2$ <b>Mxene</b>	122	1.0 M KOH	[7]
$\text{MoNiS}/\text{Mo}_2\text{TiC}_2\text{T}$ <b>x</b>	153	1.0 M KOH	[8]
<b>MX@RG</b>	121	1.0 M KOH	[9]
<b>MXene@Ce-MOF</b>	220	1.0 M KOH	[10]

**Table S3.** Comparison of the OWS activities between  $\text{Co}_2\text{V}_2\text{O}_6 \cdot 2\text{H}_2\text{O}/\text{ZIF-L}@\text{MXene}/\text{NF}$  in this work and various electrocatalysts recently reported.

Materials	$\eta_{10}$ (mV)	Electrolyte	Ref
<b>This work</b>	1.478	1.0 M KOH	<b>This work</b>
<b>CoVS NBs</b>	1.56	1.0 M KOH	[11]
<b>MOF-V-Ni<sub>3</sub>S<sub>2</sub>/NF</b>	1.58	1.0 M KOH	[12]
<b>NiCoVP</b>	1.5	1.0 M KOH	[13]
<b>V-doped CoP/NF</b>	1.53	1.0 M KOH	[14]
<b>CP-NCP-T</b>	1.54	1.0 M KOH	[15]

## References

- [1] R. Zhang, Z. Wei, G. Ye, G. Chen, J. Miao, X. Zhou, X. Zhu, X. Cao, X. Sun, "d-Electron

Complementation" Induced V-Co Phosphide for Efficient Overall Water Splitting, *Adv. Energy Mater.* 11 (38) (2021) 2101758.

- [2] W. Li, B. Feng, L. Yi, J. Li, W. Hu, Highly Efficient Alkaline Water Splitting with Ru-Doped Co-V Layered Double Hydroxide Nanosheets as a Bifunctional Electrocatalyst, *ChemSusChem* 14 (2) (2021) 730-737.
- [3] Z. Li, J. Yang, Z. Chen, C. Zheng, L.Q. Wei, Y. Yan, H. Hu, M. Wu, Z. Hu, V "Bridged" Co-O to Eliminate Charge Transfer Barriers and Drive Lattice Oxygen Oxidation during Water-Splitting, *Adv. Funct. Mater.* 31 (9) (2020) 2008822.
- [4] J. Xu, X. Zhong, X. Wu, Y. Wang, S. Feng, Optimizing the electronic spin state and delocalized electron of NiCo<sub>2</sub>(OH)/MXene composite by interface engineering and plasma boosting oxygen evolution reaction, *J. Energy Chem.* 71 (2022) 129-140.
- [5] X. Hui, P. Zhang, Z. Wang, D. Zhao, Z. Li, Z. Zhang, C. Wang, L. Yin, Vacancy Defect-Rich Perovskite SrTiO<sub>3</sub>/Ti<sub>3</sub>C<sub>2</sub> Heterostructures In Situ Derived from Ti<sub>3</sub>C<sub>2</sub> MXenes with Exceptional Oxygen Catalytic Activity for Advanced Zn–Air Batteries, *ACS Appl. Energy Mater.* 5 (5) (2022) 6100-6109.
- [6] Y. Zhang, Z. Zhang, A. Addad, Q. Wang, P. Roussel, M.A. Amin, S. Szunerits, R. Boukherroub, 0D/2D Co<sub>3</sub>O<sub>4</sub>/Ti<sub>3</sub>C<sub>2</sub> MXene Composite: A Dual-Functional Electrocatalyst for Energy-Saving Hydrogen Production and Urea Oxidation, *ACS Appl. Energy Mater.* 5 (12) (2022) 15471-15482.
- [7] Y. Hou, Z. Yuan, X. Yu, B. Ma, L. Zhao, D. Kong, Directly preparing well-dispersed ultra-hydrophilic NiFeP nanoparticle/Mxene complexes from spent electroless Ni plating solution as efficient hydrogen evolution catalysts, *J. Environ. Chem. Eng.* 11 (3) (2023) 109738.
- [8] J. Zhang, W. Zhang, J. Zhang, Y. Li, Y. Wang, L. Yang, S. Yin, MOF-derived bimetallic NiMo-based sulfide electrocatalysts for efficient hydrogen evolution reaction in alkaline media, *J. Alloys Compd.* 935 (2023) 167974.
- [9] V. Thirumal, R. Yuvakkumar, P.S. Kumar, G. Ravi, A. Arun, R.K. Guduru, D. Velauthapillai, Heterostructured two dimensional materials of MXene and graphene by hydrothermal method for efficient hydrogen production and HER activities, *Int. J. Hydrot. Energy* 48(17) (2023) 6478-6487.
- [10] S. Li, H. Chai, L. Zhang, Y. Xu, Y. Jiao, J. Chen, Constructing oxygen vacancy-rich MXene@Ce-MOF composites for enhanced energy storage and conversion, *J. Colloid Interface Sci.* 642 (2023) 235-245.
- [11] C. Wang, H. Xu, Y. Wang, H. Shang, L. Jin, F. Ren, T. Song, J. Guo, Y. Du, Hollow V-Doped CoM<sub>x</sub> (M

= P, S, O) Nanoboxes as Efficient OER Electrocatalysts for Overall Water Splitting, Inorg. Chem. 59 (16) (2020) 11814-11822.

[12] W. Dong, H. Zhou, B. Mao, Z. Zhang, Y. Liu, Y. Liu, F. Li, D. Zhang, D. Zhang, W. Shi, Efficient MOF-derived V–Ni<sub>3</sub>S<sub>2</sub> nanosheet arrays for electrocatalytic overall water splitting in alkali, Int. J. Hydrog. Energy 46 (18) (2021) 10773-10782.

[13] Y. Jeung, H. Jung, D. Kim, H. Roh, C. Lim, J.W. Han, K. Yong, 2D-structured V-doped Ni(Co,Fe) phosphides with enhanced charge transfer and reactive sites for highly efficient overall water splitting electrocatalysts, J. Mater. Chem. A 9 (20) (2021) 12203-12213.

[14] H. Xue, A. Meng, H. Zhang, Y. Lin, Z. Li, C. Wang, 3D urchin like V-doped CoP in situ grown on nickel foam as bifunctional electrocatalyst for efficient overall water-splitting, Nano Res. 14 (11) (2021) 4173-4181.

[15] D. Xu, Z. Kang, H. Zhao, Y. Ji, W. Yao, D. Ye, J. Zhang, Coupling heterostructured CoP-NiCoP nanopin arrays with MXene (Ti<sub>3</sub>C<sub>2</sub>T<sub>x</sub>) as an efficient bifunctional electrocatalyst for overall water splitting, J. Colloid Interface Sci. 639 (2023) 223-232.